



UNIVERSITATEA BABEȘ-BOLYAI
BABEȘ-BOLYAI TUDOMÁNYEGYETEM
BABEȘ-BOLYAI UNIVERSITÄT
BABEȘ-BOLYAI UNIVERSITY

FACULTATEA DE FIZICĂ
Str. Mihail Kogălniceanu nr.1
Cluj-Napoca, RO-400084
Tel: +4(0)264-405300 | FAX: +4(0)264-591906
secretariat.phys@ubbcluj.ro
www.phys.ubbcluj.ro



DOCTORAL SCHOOL OF PHYSICS

SUMMARY OF THE DOCTORAL THESIS

PhD student
Ana Maria Raluca GHERMAN

Supervisor
Prof. Vasile CHIȘ

July 2022
Cluj-Napoca



UNIVERSITATEA BABEȘ-BOLYAI
BABEȘ-BOLYAI TUDOMÁNYEGYETEM
BABEȘ-BOLYAI UNIVERSITÄT
BABEȘ-BOLYAI UNIVERSITY

FACULTATEA DE FIZICĂ
Str. Mihail Kogălniceanu nr.1
Cluj-Napoca, RO-400084
Tel: +4(0)264-405300 | FAX: +4(0)264-591906
secretariat.phys@ubbcluj.ro
www.phys.ubbcluj.ro



DOCTORAL SCHOOL OF PHYSICS

Cheminformatics tools used to characterize the structure and bactericidal-activity of β -lactams against pathogens

PhD student

Ana Maria Raluca GHERMAN

Supervisor

Prof. Vasile CHIȘ

July 2022
Cluj-Napoca

THESIS'S TABLE OF CONTENTS

Table of contents	4
Introduction	7
Part I. Bacteria	10
Chapter 1. Multivariate analysis	12
Theory and motivation	13
Computational details	18
Results and discussion	18
1. <i>Enterococcus faecalis</i> samples following different sample preparation protocols	18
PCA on full spectrum	20
PCA on NPs' response	21
PCA on the bacterial fingerprint	22
PCA-LDA	23
2. Gram-negative – Gram-positive discrimination	25
2.1 GN <i>Pseudomonas aeruginosa</i> vs. GP <i>Enterococcus faecalis</i> and <i>Staphylococcus aureus</i>	25
2.2 GN <i>Aeromonas hydrophila</i> vs. GP <i>Bacillus cereus</i> samples	29
2.3 A mix of GN <i>Aeromonas hydrophila</i> vs. GP <i>Bacillus cereus</i> samples	31
3. SERS-PCA based alternative resistogram	34
4. DNA samples of <i>Salmonella serovars</i> UV irradiated	36
Conclusions	41
Chapter 2. Raman technique and Density Functional Theory – the 'R'&'D' in Research and Development of antibiotics	44
Theory and motivation	45
Raman spectroscopy	45
Density Functional Theory (DFT)	46
Hohenberg-Kohn Theory	46
The first Hohenberg-Kohn theorem	46
The second Hohenberg-Kohn theorem	46
The Kohn-Sham equations	47
Density Functionals	47
Local density approximation (LDA)	47
Gradient corrected functional	48
Computational details	48
Results and discussions	49
1. Vibrational spectra	49
1.1 Common bands	51
1.2 Specific bands	52
2. Molecular Electrostatic Potential surfaces (MEPs)	58
3. Frontier molecular orbital (FMO) studies	59
Chapter 3. Can molecular docking solely predict antibiotics' bactericidal activity?	64
Theory and motivation	65
The theory behind molecular docking	65
B-lactams' mechanism of action	66
B-lactams' classification	66
Computational details	69
Selecting the ligands and receptors	69

Building the ligand-receptor complexes	69
Setting the search box	69
Running the code	70
Results and discussions	72
1. Molecular docking	72
2. Disk diffusion tests	80
Conclusions	83
Part II. Fantastic yeasts and where to find them	85
Theory and motivation	86
Results and discussion	88
1. Principal Component Analysis (PCA)	88
2. Linear Discriminant Analysis (PCA-LDA)	92
3. DFT calculations	95
Conclusions	99
Overview	101
Acknowledgements	103
Abbreviations	105
References	106
Dissemination of the results	111
ADDENDUM 1 - Full assignments of the common FT-Raman bands observed for benzypenicillin, oxacillin, ampicillin, carbenicillin, and azlocillin	114
ADDENDUM 2 - List of hydrogen bonds formed between the most stable conformer of each ligand and surrounding residues in PBPs	122
ADDENDUM 3 - List of samples chosen for training and testing sets of Models I-X	128

Summary

Rapid pathogen detection and identification are critical for public health. Traditional microbiological diagnostic procedures have reached their physical limitations, with severe repercussions, particularly in children (e.g. hemolytic uremic syndrome, sepsis). One of the constraints is the extensive time (in the order of days) required for pathogen identification at the strain level. On the other hand, as surgery (e.g. transplants, neonatal surgery) and emergency medicine advanced, so did severe postoperative complications such as nosocomial infections leading to septic shock in the absence of targeted treatment. Hospital-acquired bacterial infections are unfortunately widespread in Romania (1, 2) and create a critical problem since delays in proper initial antimicrobial therapy are known to dramatically increase morbidity. Infection control measures such as screening protocols for patients at high risk, isolation/precautionary protocols for patients identified as culture-positive for high-risk pathogens, decontamination protocols, and appropriate microbiological screening procedures such as periodic sensitivity testing are conventional strategies to prevent and overcome this scenario, but they are not efficient and reliable in the long term (3).

Antimicrobial resistance (AMR) is defined as microbes' capacity to withstand antibiotic actions, limiting treatment choices and increasing the costs and potential side effects for patients. Practically, these organisms have concurrently evolved mechanisms of antimicrobial resistance, and the medical community is losing an arms race with infectious organisms that were once simple to treat (4, 5). Due to economic constraints, diagnostic test availability, much of the research investigating AMR rates has been based on single organisms within certain global regions (4). The main antibiotic-resistant pathogens (ARP) are: *Escherichia coli*, *Pseudomonas aeruginosa*, *Candida albicans*, methicillin-resistant *Staphylococcus aureus* (MRSA), vancomycin-resistant *Enterococci* (VRE), *Acinetobacter baumannii*, penicillin-resistant *Streptococcus pneumoniae* (PRSP), extensively drug-resistant (XDR) *Mycobacterium tuberculosis*, extended-spectrum β -lactamase-producing *Enterobacteriaceae*, and *Klebsiella pneumoniae*. In 2014, the World Health Organization (WHO) published the most comprehensive surveillance report to date (6), which analyzes resistance rates of common infections from 114 countries. The economic effort in the USA alone costs over \$20 billion healthcare expenses per year only for treating the 1.7 million hospital associated infections (HAI), which also lead to 99,000 possibly preventable deaths. This is the case in a country in which antimicrobial resistance rates are far lower and the antimicrobials are significantly more accessible than in any other country (7).

Recently, spectroscopic techniques have become more promising due to the development of low-cost, label-free and ultrasensitive detection methods, allowing for rapid, specific and sensitive enough results as to be applied in critical areas such as healthcare. Raman spectroscopy is a non-invasive *in situ* analysis method that requires little sample preparation and that can also be easily utilized outside the scientific laboratory by using the portable, miniaturized, even handheld versions of Raman spectrometers (7-10). When using the surface-enhanced Raman scattering (SERS) effect, it may achieve single-molecule sensitivity (11). Due to the massive amplification in a SERS experiment (up to 10^{10}), traces of closely adsorbed molecules on metallic nanostructures, usually nanoparticles (NPs), can be detected.

The present work is divided into two parts, each dealing with one of the two main classes of pathogens – bacteria (**Part I**) and fungi (**Part II**).

Part I tells the beginning of the story of the “Cheminformatic tools used to characterize the structure and bactericidal-activity of β -lactams against pathogens”. It began in 2014, when Dr. Nicoleta Dina,

the head of the small scientific team I am currently a part of, together with another group of researchers from Deutschland developed a new method of bacterial detection by using SERS (12-18). After optimizing the detection method in the lab, the team aimed to find way to make it more accessible to society, having as a final target to implement the methodology in the medical system as an alternative for pathogen detection. Thus, in 2017, the experimentalists of our team developed a demonstrator which could be implemented in the medical system. The proposed nano-screening platform offers a unique approach that is different from other medical techniques utilized nowadays for the screening of pathogens in routine clinical work. It combines SERS for the ultrasensitive molecular fingerprinting of pathogens with microfluidics for their isolation (19).

Chemometrics, the most employed cheminformatics tool in **Chapter 1. Multivariate analysis**, has previously been incorporated with spectroscopic instrumentation as a standard for easing spectral data interpretation by employing linear algorithms such as Principal Component Analysis (PCA), Linear Discriminant Analysis (LDA), etc (20-25).

Principal Component Analysis (PCA) is a statistical method, extensively used nowadays, for analysing big data; it emphasizes variation and brings out strong patterns. It is also used for designing prediction models. One of its particularities is dimensionality reduction. Thus, PCA is a suitable tool for analysing vibrational spectra, particularly SERS fingerprints of microorganisms.

An alternative to PCA is the Linear Discriminant Analysis (LDA), a supervised, simple and robust method. The LDA aims to predict the samples from a data set into already known classes. Like PCA, LDA aims to reduce the number of variables used when creating a model by projecting the samples of interest into a new coordinate system so as to maximize the distance between classes (by maximizing the distance between the mean values of each class). At the same time, it aims to minimize the variability within a class (reducing the dispersion of samples belonging to the same class). When the PCs previously calculated for PCA are used as variables in LDA, the resulting method is called PCA-LDA.

The purpose of the following work is to demonstrate how multivariate data analyses can be employed to discriminate between pathogens at strain level by highlighting their similarities and differences, including after following different sample preparation protocols. The results of such big data analysis tool are a strong indicator of its huge potential for fast, accurate, and reliable analysis with promising potential in clinical applications, such as designing SERS-PCA antibiogram employed for targeted antibiotherapy.

Several discrimination and classification models have been designed by employing PCA and PCA-LDA, respectively. In designing these models, we aimed to find specific spectral features for SERS response in different situations, such as: samples were prepared by using different protocols ("*E. faecalis* samples following different sample preparation protocols" section), samples belong to one of the two Gram-positive and Gram-negative classes ("*GN Pseudomonas aeruginosa* vs. GP *Enterococcus faecalis* and *Staphylococcus aureus*" and "*GP Bacillus cereus* vs. GN *Aeromonas hydrophila*" sections), samples come from a mixture of two species ("*A mix of GP Bacillus cereus* and GN *Aeromonas hydrophila* samples" section), or they are treated with antibiotics to which they are sensitive or resistant ("*SERS-PCA based alternative resistogram*" section), and, finally, irradiated DNA samples of *Salmonella* serovars ("*DNA Salmonella* serovars UV irradiated" section). SERS spectra of bacteria were recorded on *Aeromonas hydrophila*, *Bacillus cereus*, *Enterococcus faecalis*, *Pseudomonas aeruginosa*, *Staphylococcus aureus*, and DNA samples of *Salmonella* serovars.

The discrimination model built on *Enterococcus faecalis* samples from three different sample preparation methods (in mixture with *a priori* synthesized AgNPs by Leopold-Lendl or Lee Meisel recipe, and with *in situ* synthesized AgNPs at their cell wall) found that the 728cm^{-1} SERS band contributed the most to the differentiation. The classification model was able to predict the sample preparation protocols with an accuracy and sensibility of 95%, and a precision and specificity of 97%. Two models were developed when we aimed to discriminate between Gram-positive and Gram-negative samples. For the discrimination model containing *Staphylococcus aureus*, *Enterococcus faecalis*, and *Pseudomonas aeruginosa*, we obtained a total variance of 75%, whereas the classification model had an accuracy of 96%. As for the database containing *Aeromonas hydrophila* and *Bacillus cereus* samples, the maximum variation added by the first three PCs is 87%.

When aiming to discriminate between unknown labels in a mix of two species, for the database containing the same *Aeromonas hydrophila* and *Bacillus cereus* samples but in a mix, we have obtained a discrimination of 74%. The model was checked with known samples (blind test), and for the validation model, we got a better total variance of 79%.

On the database containing *Aeromonas hydrophila* samples without treatment, treated with an antibiotic to which it shows resistance (carbenicillin) and one to which it shows sensitivity (azlocillin), a SERS-PCA-based alternative resistogram was proposed as a clinically useful insight from a study of carbenicillin and azlocillin that used both cheminformatics and vibrational analysis together. The maximum variance obtained for the discrimination model was 84%.

DNA samples of *Salmonella* serovars UV irradiated at different time intervals; samples belonging to the same serovar clustered together even after irradiation.

The Raman experimental technique provides molecular specific information including the geometrical and electronic structural aspects in the form of fingerprint-like spectra. Even though each molecule has a unique spectrum, a precise assignment is very challenging, particularly for medium and large-sized molecules. Subtle features' description of the spectroscopical data requires sophisticated theoretical tools and considerable computational resources (CPU time and memory).

Thanks to the impressive development of hardware and software technology, quantum chemical computations have been rapidly integrated as a fundamental tool in support of the experimental approaches. The computational infrastructure at Babeş-Bolyai University allows for high-level quantum chemical calculations on large-sized molecular systems by the UBB cluster and the accuracy of Density Functional Theory methods, thus assigning subtle features of experimental Raman spectra of large molecular systems is now possible for UBB scientists as well.

The extensive use and/or the misuse of antibiotics caused multidrug resistance after a period of intensive use. As a consequence, it is critical to development new and more effective antibiotics. Understanding the geometrical and electronic structure of such molecules is a must when it comes to designing new drugs. This provides valuable information for further investigations of specific drug-pathogen chemical reactions, such as the bonding mechanism of an antibiotic to a specific component of the bacterial cell-wall in order to have a bactericidal effect.


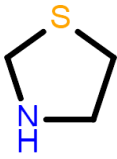
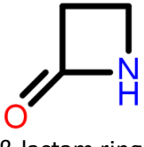
The Raman experimental technique provides molecular information specific to electronic and structural aspects in the form of fingerprint-like spectra, unique for each molecule, which makes it suitable for detailed characterization of antibiotics from this point of view. The Raman study in **Chapter 2. Raman technique and Density Functional Theory – the 'R'&'D' in Research and Development of antibiotics** includes one antibiotic from each of the five classes of penicillins – benzylpenicillin (BPN), oxacillin (OXN), ampicillin (APN), carbenicillin (CBN), and azlocillin (AZN). The

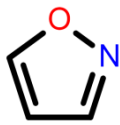
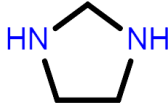
similarities in the Raman spectra are explained by the penam-core, the shared component in their molecular structure. On the other hand, various R side-chains bound to the penam core give the Raman response in the form of subtle features.

Quantum chemical frequency calculations were employed by using Gaussian software package (20) on all five penicillins in order to explain their Raman response by a full assignment of the bands. Theoretical Raman spectra were obtained at both harmonic and anharmonic approximations.

Due to their common chemical structure – a benzene, a thiazolidine and a β -lactam ring, two methyl and two carbonyl groups, a carboxyl and an amide group, in their structure, penicillins come with a specific Raman response, 1002-1004 cm^{-1} being the most intense band in all spectra. The most intense bands of the methyl groups is the doublet 1433-1437/1452-1459 cm^{-1} , whereas the doublet 870-876/894-895 cm^{-1} , is the most intense response of the carboxyl group. The deformation of thiazolidine ring can be observed at 571-579 cm^{-1} , while the response of the β -lactam ring is the most intense at 1156-1158 cm^{-1} and 1158-1175 cm^{-1} . Specific marker bands for each antibiotic – BPN, OXN, APN, CBC, and AZL - are present in their spectra as expected, but most of the Raman response is subtle, having weak and very weak intensity. OXN's Raman spectrum stands out the most, due to the increased intensity of 1606 cm^{-1} (C6C7 stretching), as well as 1444 (CH_3 bending) and 1471 cm^{-1} (C=N and CC stretchings). APN's Raman spectrum comes with more visible differences as well – 780 cm^{-1} (NH bending) and 830 cm^{-1} (NH_2 twisting).

Table 1 – Experimental (1064 nm) Raman marker bands of penicillins (common to all five penicillins) and specific Raman bands for BPN, OXN, APN, CBC, and AZL molecules classified by chemical groups.

Chemical group	BPN		OXN		APN		CBC		AZL		common bands	
 benzene ring	621	839	629	845	615	830	617	834	617	-		
	983	1002	982	1002	993	1003	957	1004	988	1003		
	1029	1582; 1600	1026	1578; 1606	1027	1585; 1602	1032	1582; 1600	1030	1585; 1602		
CH_3 methyl group	231	960	250	-	240	951;	246	948	241	948;		
	274	1436	279	1433	271	961	280	1436	-	958		
	292	1452;	296	1459	291	1435	-	1457	294	1437		
		1468				1456				1458		
COOH carboxyl group	360	873+895	368	894;	360	873;	361	876;891	360	870;899		
	-	919	522	910	522	910	525	920	-	-		
	807	1245	-	920	802	-	803	-	-	-		
	-		-	-	847	1249	847	-	850	-		
NH amide group	661		656		670		666		661			
	1178		-		1178		-		1175			
C=O carbonyl group	402		406		409		405		409			
	1638		1649		1693		1666		1660			
 thiazolidine ring	571		579		-		577		575			
	602		616		601		602		-			
	919		920		926		920		913			
	1292		-		-		1297		-			
 β -lactam ring	945		944		-		-		-			
	-		-		1156		1156		1158			
	1775		1758		1764		1763		1775			
CH_2	468		x		x		x		x		p s	

methylene group	1419								
 isoxazole ring	x	250 336 492 648 734 793	908 1308 1444 1471 1516 1556	x	x	x			
NH ₂ amino group	x	x		465 830 1119	1186 1512 1638	x	x		
COOH carboxyl group	x	x				666 746 1126	1180 1372 1666 1763	x	
 imidazolidine ring	x	x		x		x		465 714 958	1125 1239 1397
NH amide group	x	x		x		x		641 1532	

Antibiotics's reactivity was also described by Frontier Molecular Orbitals (FMO) and the resulted reactivity descriptors as well as Molecular Electrostatic Potential surfaces (MEPs). All calculations were performed by using Density Functional Theory (DFT) methods.

It is clear that for all compounds, the most electronegative sites are concentrated on the O atoms in carbonyl groups, whereas the most electropositive sites are localized on the N atoms. In addition, another electronegative area in OXN's MEP is located on O and N atoms of the isoxazole ring; for APN, electronegative sites are located on the O atom in the second carboxyl's hydroxyl as well as on the amide's N atom. In CTR's MEP, a second electronegative area is located on the O atom in the β -lactam ring.

By taking into account the scored values for both their electronegative and electropositive sites on the MEP, out of the selected compounds – BPN, OXN, APN, CBC, AZL, CFZ, CFP, CRT – the three cephalosporins turn out to present higher reactivity as acceptors than the selected penicillins, whilst as donors, CTR, CFZ and CBC with similar reactivity toward surrounding electros, followed by CFP and AZL.

Frontier molecular orbitals (FMOs), which include the highest occupied molecular orbital (HOMO) and the lowest unoccupied molecular orbital (LUMO), provide information on a molecule's chemical reactivity and stability. Figure 1 illustrates the distribution of the charges in the FMOs of the antibiotics of interest – BPN, OXN, APN, CBC, AZL, CFZ, CFP, and CTR, with the negative (red) and positive (green) values of the orbitals. Their energy levels and the (HOMO-LUMO) band gap (HLG) are also indicated in each case.

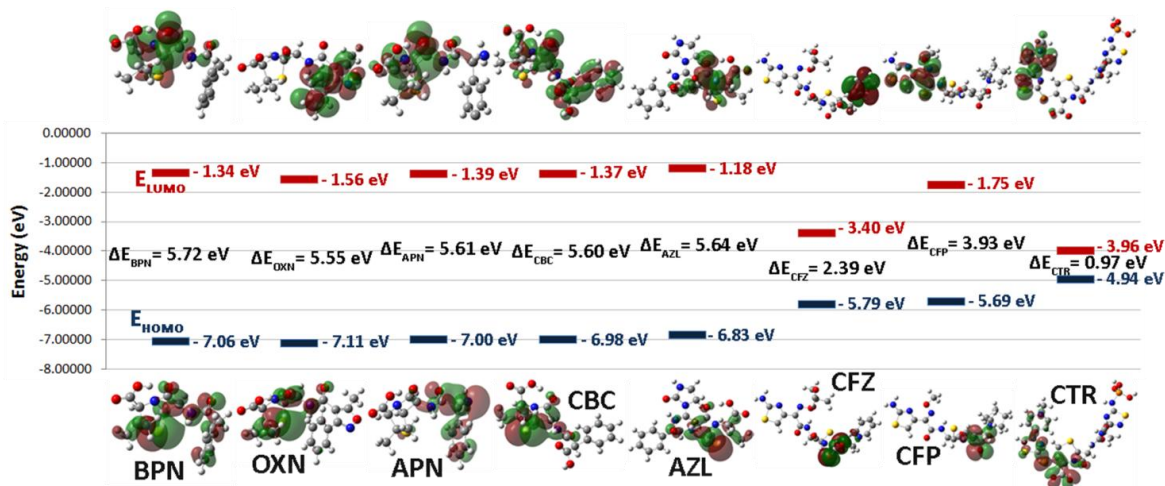


Figure 1 - FMO diagrams for benzylpenicillin (BPN), oxacillin (OXN), ampicillin (APN), carbenicillin (CBC), azlocillin (AZL), ceftazidime (CFZ), cefepime (CFP), and ceftaroline (CTR) calculated at B3LYP/6-311+G(2d,p) level of theory. Types of atoms: carbon – grey; nitrogen – blue; oxygen – red; sulfur – yellow; phosphorus – orange; hydrogen – white.

Together with Koopmans's theory (21), which states a molecule's first ionization energy is equal to the negative value of the HOMO's energy, several parameters have been described over time for a better characterization of a compound's chemical reactivity, such as ionization potential (I), electron affinity (A), (HOMO-LUMO) band gap (HLG), global hardness (η) and softness (σ) (22), electronegativity (χ) (23) and its reverse, the chemical potential (μ), and the global electrophilicity index (ω) (24, 25). All of the previously mentioned parameters are calculated for both penicillin class compounds - BPN, OXN, APN, CBC, and AZL – and cephalosporin class compounds - CFZ, CFP, and CTR. Table 2 summarizes their calculated values.

Table 2 – Quantum chemical reactivity descriptors obtained on the optimized geometries of the selected antibiotics by DFT calculations in gas phase at B3LYP/6-311+G(2d,p) level of theory. All values are in eV.

Descriptor	Equation	Penicillins					Cephalosporins		
		BPN	OXN	APN	CBC	AZL	CFZ	CFP	CTR
E_{HOMO}		-7.06	-7.11	-7.00	-6.98	-6.83	-5.79	-5.69	-4.94
E_{LUMO}		-1.34	-1.56	-1.39	-1.37	-1.18	-3.40	-1.75	-3.96
I (ionization potential)	$I = -E_{HOMO}$	7.06	7.11	7.00	6.98	6.83	5.79	5.69	4.94
A (electron affinity)	$A = -E_{LUMO}$	1.34	1.56	1.39	1.37	1.18	3.40	1.75	3.96
HLG (HOMO-LUMO gap)	$HGL = E_{HOMO} - E_{LUMO} $	5.72	5.55	5.61	5.60	5.64	2.39	3.93	0.97
η (global hardness)	$\eta = \frac{I - A}{2}$	2.86	2.77	2.80	2.80	2.82	1.19	1.96	0.48
σ (global softness)	$\sigma = \frac{1}{\eta}$	0.34	0.35	0.35	0.35	0.35	0.83	0.50	2.04
χ (electronegativity)	$\chi = \frac{I + A}{2}$	4.20	4.34	4.20	4.18	4.00	8.82	3.52	20.35
μ (chemical potential)	$\mu = -\frac{I + A}{2}$	-4.20	-4.34	-4.20	-4.18	-4.00	-4.59	-3.72	-4.45
ω (global electrophilicity index)	$\omega = \frac{\mu^2}{2\eta}$	3.08	3.39	3.14	3.11	2.84	4.59	3.72	4.45

Overall, looking at the global reactivity descriptors in Table 8, the eight β -lactam antibiotics may be ordered from most likely to least likely to exhibit bactericidal properties as follows: if ω values are considered, CFZ>CTR>CFP>OXN>APN>CBC>BPN>AZL; for HGL and σ , CTR>CFZ>CFP>OXN>CBC>APN>AZL>BPN; for the ionization potential I, OXN>BPN>APN>CBC>AZL>CFZ>CFP>CTR; lastly, if taking into account their electronegativity χ , the order is CTR>CFZ>OXN>BPN>APN>CBC>AZL>CFP. The antibiotic with the strongest bactericidal activity should have the lowest HLG and the highest I and ω . Thus, in the penicillin class, OXN exhibits the most potent bactericidal activity, but the rest of the penicillins scored close values for their reactivity descriptors as well. The CTR and CFZ cephalosporins, on the other hand, are significantly more reactive than the other tested β -lactams.

By using DFT frequency calculations, we aimed to reveal the (dis)similarities in the chemical structures of five penicillins – benzylpenicillin, oxacillin, ampicillin, carbenicillin, and azlocillin. We identified the specific Raman response of penicillins as being band at 1002-1004 cm^{-1} . On the other hand, the specific Raman marker bands of each antibiotic are only subtle. Oxacillin's Raman spectrum stands out the most, having the marker bands at 1606 cm^{-1} , 1444 cm^{-1} , and 1471 cm^{-1} . By combining Frontier Molecular Orbital (FMO) and Molecular Electrostatic Potential surface (MEP) studies, we have identified oxacillin as having the highest potential for being a bactericidal agent due to its chemical reactivity. Carbenicillin, a 4th generation penicillin, came in as the second best bactericidal compound.

When looking for a novel pharmaceutical, a cheaper, more accessible and rapid alternative to high-throughput assays based on a sophisticated and interdisciplinary technology that is often only available to large pharmaceutical companies is molecular docking. It is a cheminformatics tool used for virtual screening of active compounds in order to determine the hits from the leads.

In **Chapter 3 - Can molecular docking solely predict antibiotics' bactericidal activity?**, the purpose of the study was to determine the antibiotic(s) most effective against different Gram-positive and negative bacteria. The antibiotics under consideration are two types of beta-lactams – penicillins and cephalosporins. One penicillin of each generation – benzylpenicillin (BPN), oxacillin (OXN), ampicillin (APN), carbenicillin (CBC), and azlocillin (AZN), as well as cephalosporins one for each 3rd, 4th and 5th generations - ceftazidime (CFZ), cefepime (CFP), and ceftaroline (CTR) were selected for the *in silico* structure – action mechanism relationship.

In this study, the best conformers of each antibiotic was identified by considering the geometric specificity, the binding energy, and the interaction with target's residues. In the end we were able to name the best candidates as bactericidal agents from the conformational structure point of view.

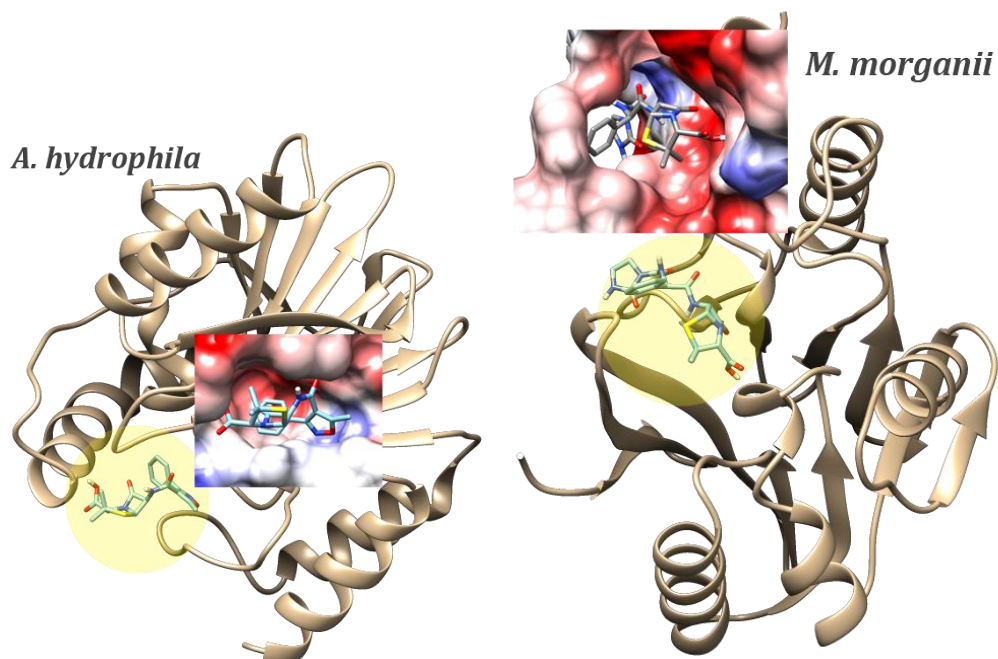


Figure 2 – Position of the binding sites of PBPs from GN *A. hydrophila* (PDB id: 1x8i) in complex with OXN which scored the lowest binding energy (-8.8 kcal/mol), and *M. morganii* (PDB id: 6l3s) in complex with AZL conformer which scored the lowest binding energy (-8.0 kcal/mol). Zoomed-in pictures show the Coulombic electrostatic surface of the binding sites.

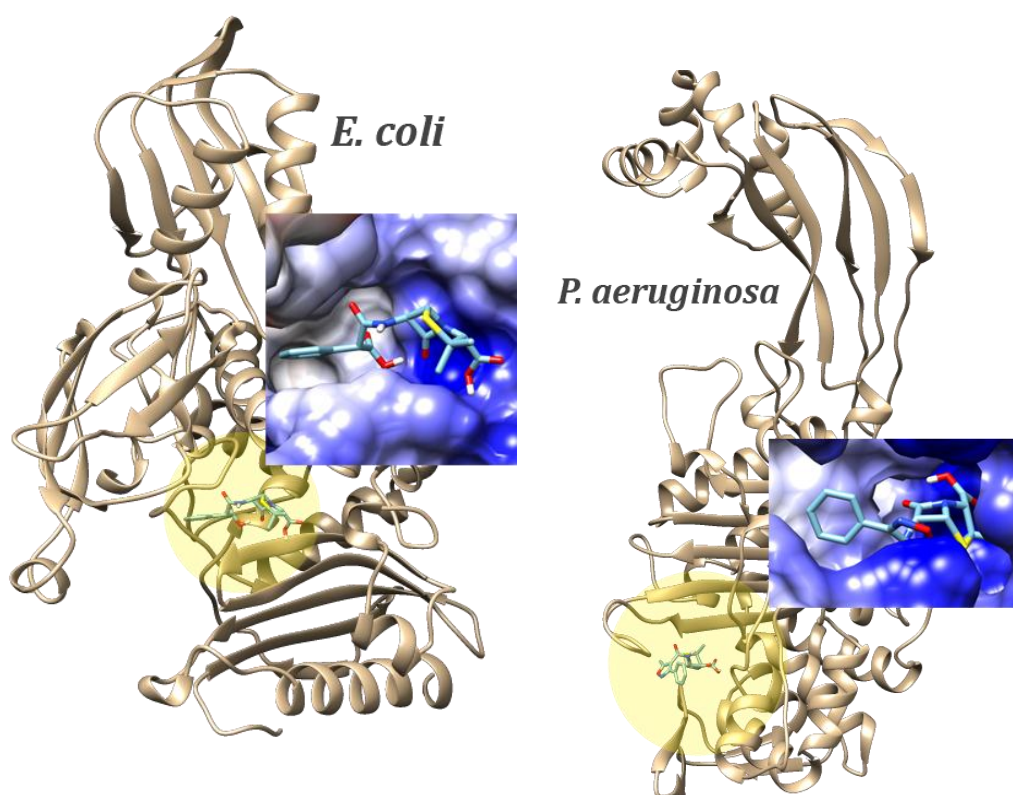


Figure 3 – Position of the binding sites of PBPs from GN *E. coli* (PDB id: 2ex6) in complex with OXN conformer (top) which scored the lowest binding energy (-8.6 kcal/mol) and *P. aeruginosa* (PDB id: 5df7) in complex with OXN conformer (bottom) which scored the lowest binding energy (-10.3 kcal/mol). Zoomed-in pictures show the Coulombic electrostatic surface of the binding sites.

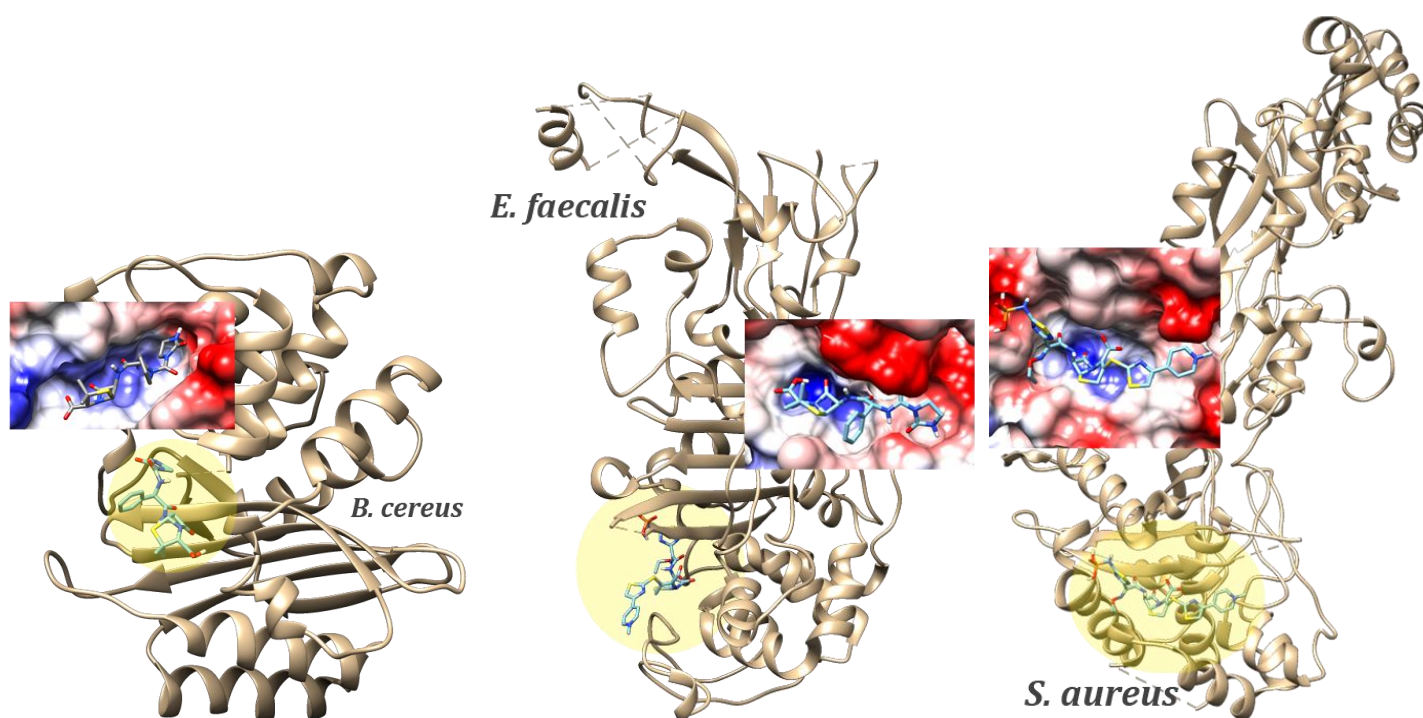


Figure 4 – Position of the binding sites of PBPs from GP *B. cereus* (PDB id: 6w33) in complex with AZL conformer, which scored the lowest binding energy (-8.6 kcal/mol) and *E. faecalis* (PDB id: 6mkh) in complex with CTR conformer, which scored the lowest binding energy (-8.8 kcal/mol) and GP *S. aureus* (PDB id: 6h5o) in complex with CTR conformer, which scored the lowest binding energy (-8.2 kcal/mol). Zoomed-in pictures show the Coulombic electrostatic surface of the binding sites.

Disk diffusion tests were employed on Gram-positive and Gram-negative bacteria to determine if molecular docking alone can predict the bactericidal activity. The inhibition zones are listed in Table 4.

The lowest binding energies scored by each ligand as well as the average value of the first binding energies in each code run are listed in Table 3.

Table 3 - Minimum and average binding energy (in kcal/mol) of best conformer from each code run of penicillins (BPN, OXN, APN, CBC, and AZL) and cephalosporins (CFZ, CFP, CTR) docked to PBPs (PDB id's in parenthesis) from *A. hydrophila*, *M. morgani*, *E. coli*, *P. aeruginosa*, *B. cereus*, *E. faecalis* and *S. aureus*. The average binding energies including the standard deviations, are plotted below.

Class	Pathogen	Penicillins					Cephalosporins		
		BPN	OXN	APN	CBC	AZL	CFZ	CFP	CTR
GN	<i>A. hydrophila</i> (1x8i)	-8.0 -7.83±0.21	-8.8 -8.70±0.02	-7.7 -7.51±0.08	-8.3 -8.20±0.10	-8.3 -7.95±0.19	-	-	-
	<i>M. morgani</i> (6l3s)	-7.4 -7.13±0.13	-8.0 -7.81±0.06	-7.3 -7.16±0.07	-7.6 -7.40±0.16	-8.0 -7.86±0.08	-	-	-
	<i>E. coli</i> (2ex6)	-7.8 -7.74±0.05	-8.6 -8.59±0.04	-7.5 -7.44±0.05	-8.2 -8.13±0.05	-8.1 -7.96±0.15	-7.7 -7.70±0.02	-7.6 -7.08±0.44	-8.0 -7.71±0.26
	<i>P. aeruginosa</i> (5df7)	-9.1 -8.22±0.45	-10.3 -9.85±0.46	-8.4 -8.07±0.23	-8.8 -8.63±0.19	-9.6 -9.42±0.06	-9.6 -9.44±0.25	-8.1 -8.05±0.05	-9.1 -8.77±0.17
GP	<i>B. cereus</i> (6w33)	-7.6 -7.26±0.14	-8.5 -8.06±0.13	-7.7 -7.51±0.10	-8.2 -8.09±0.06	-8.6 -8.32±0.12	-	-	-
	<i>E. faecalis</i> (6mkh)	-7.9 -7.61±0.20	-7.8 -7.70±0.03	-7.5 -7.27±0.09	-7.7 -7.50±0.10	-8.6 -8.44±0.18	-8.5 -8.46±0.05	-7.8 -7.80±0.00	-8.8 -8.66±0.11
	<i>S. aureus</i> (6h5o)	-7.5 -7.04±0.38	-7.7 -7.06±0.23	-7.5 -7.15±0.15	-8.0 -7.80±0.10	-7.9 -7.58±0.15	-7.8 -7.50±0.17	-7.5 -7.50±0.00	-8.2 -7.91±0.43

Table 4 – Inhibition zones to the selected antibiotics for pathogens belonging to both Gram-negative (GN) - *Aeromonas hydrophila* PAI-45 and PI-88, *Morganella morganii* PI-81, *Pseudomonas aeruginosa* ATCC 27853, and Gram-positive (GP) classes - *Bacillus cereus* ESN-09, *Enterococcus lactis* CE-13, *Enterococcus durans* CI-28 (GP), *Staphylococcus aureus* ATCC 25923, and *Micrococcus luteus* DSM 20030. Inhibition areas are in mm, while R means “resistant”.

Class	Pathogen	Penicillins					Cephalosporins		
		BPN	OXN	APN	CBC	AZL	CFZ	CFP	CTR
GN	<i>A. hydrophila</i> PAI-45	R	R	R	R	14.3	-	-	-
	<i>A. hydrophila</i> PI-88	R	R	14.2	20.7	14.5	-	-	-
	<i>M. morganii</i> PI-81	R	R	R	R	R	-	-	-
	<i>P. aeruginosa</i> ATCC 27853	R	R	-	-	-	24.0	28.6	23.0
GP	<i>B. cereus</i> ESN-09	R	R	R	R	R	-	-	-
	<i>E. lactis</i> CE-13	14.7	R	22.7	14.2	18.7	-	-	-
	<i>E. durans</i> CI-28	16.3	R	24.0	16.1	20.1	-	-	-
	<i>S. aureus</i> ATCC 25923	32.7	26.6	-	-	-	16.2	25.5	29.7
	<i>M. luteus</i> DSM 20030	-	-	-	-	-	34.8	43.3	39.6

The key outcomes of the Molecular Docking studies demonstrated that both a newer generation antibiotic (azlocillin) and an older generation antibiotic (oxacillin) are effective against various penicillin-binding proteins from GP and GN bacteria. OXN scored the strongest binding energies to *Aeromonas hydrophila* (GN) (-8.70 ± 0.02 kcal/mol) and *Morganella morganii* (GN) (-7.86 ± 0.08 kcal/mol), whereas AZL scored the strongest binding energies to *Bacillus cereus* (GP) (-8.32 ± 0.12 kcal/mol) and *Enterococcus faecalis* (-8.44 ± 0.18 kcal/mol). Their bactericidal activity was tested and confirmed on a couple of both GP and GN species by using the disk diffusion method. Additionally, a SERS – PCA based resistogram of *Aeromonas hydrophila* is proposed as a clinically relevant insight resulting from the synergistic cheminformatics and vibrational study on CBC and AZL.

Finally, in **Part II**, based on a collection of SERS fingerprints of three *Candida* species, we aimed to develop a molecular diagnosis method for fungal infections by combining surface-enhanced Raman scattering, multivariate analyses such as PCA and LDA-PCA, and accurate computational spectroscopy tools. This effort represents the first steps towards enabling early detection of pathogenic resistance, which holds great promise as rapid, reliable, competitive and cost-effective alternative for infection screening and treatment.

PCA was performed on a database containing SERS spectra of *Candida* species. We have developed a classification model containing three different species - *Candida albicans*, *Candida glabrata*, and *Candida parapsilosis*. Due to the shortage of real samples, data augmentation tools were used to extend the database. The method comprises a discrimination and a classification model. The classification model has 95% accuracy. It was also described by 98% precision, 95% sensitivity, and 97% specificity.

We also identified the SERS marker bands responsible for species discrimination. Furthermore, we went a step further in determining the origins of these marker bands. We already know that SERS signal is specific to the fungi cell wall. As a result, several of its key components' specific SERS (N-acetylglucosamine, β -1,3-glucan, β -1,6-glucan, and mannose) should be present.

For the first time, we obtained the calculated Raman spectra for N-acetylglucosamine, β -1,3-glucan, β -1,6-glucan, and mannose. Following that, we explained in detail how these cell wall components' Raman bands correlate to the SERS spectra of the three *Candida* species.

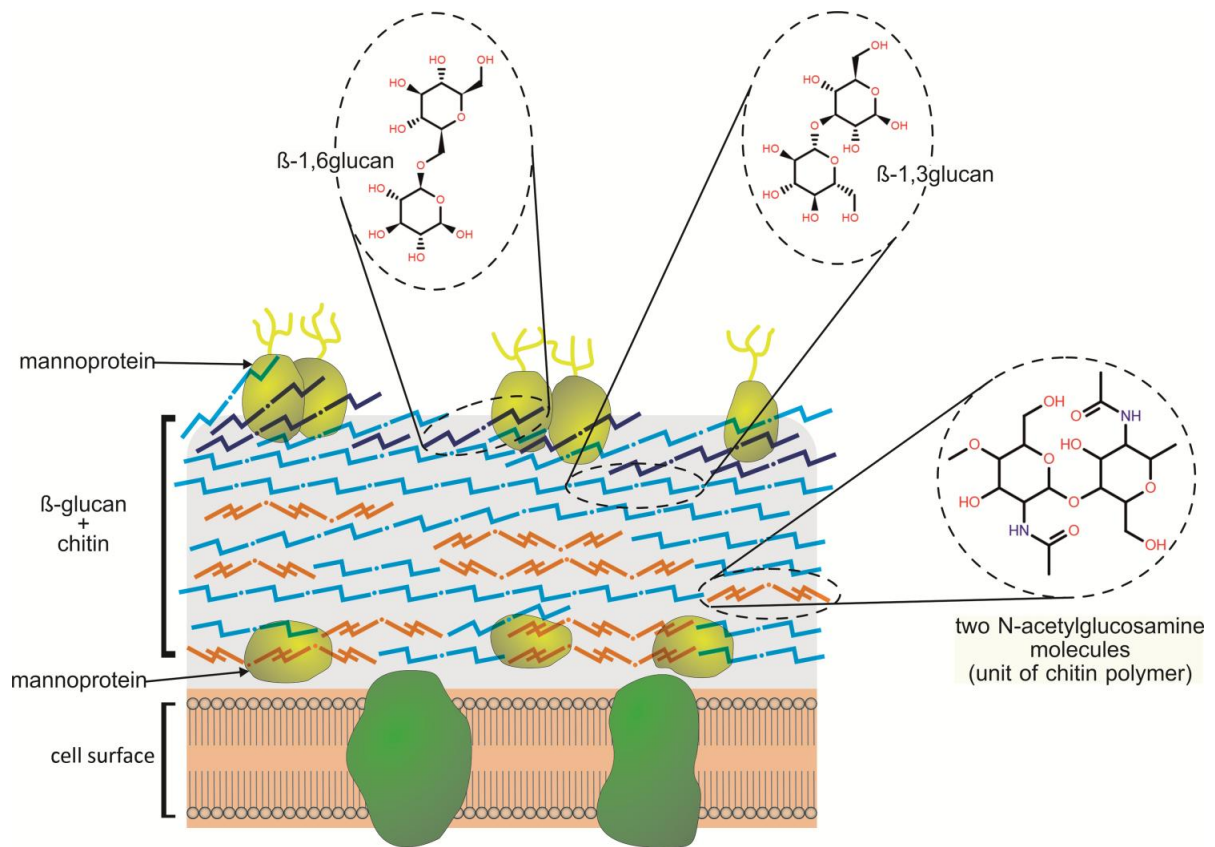


Figure 5 – Cell wall structure and main components of yeast.

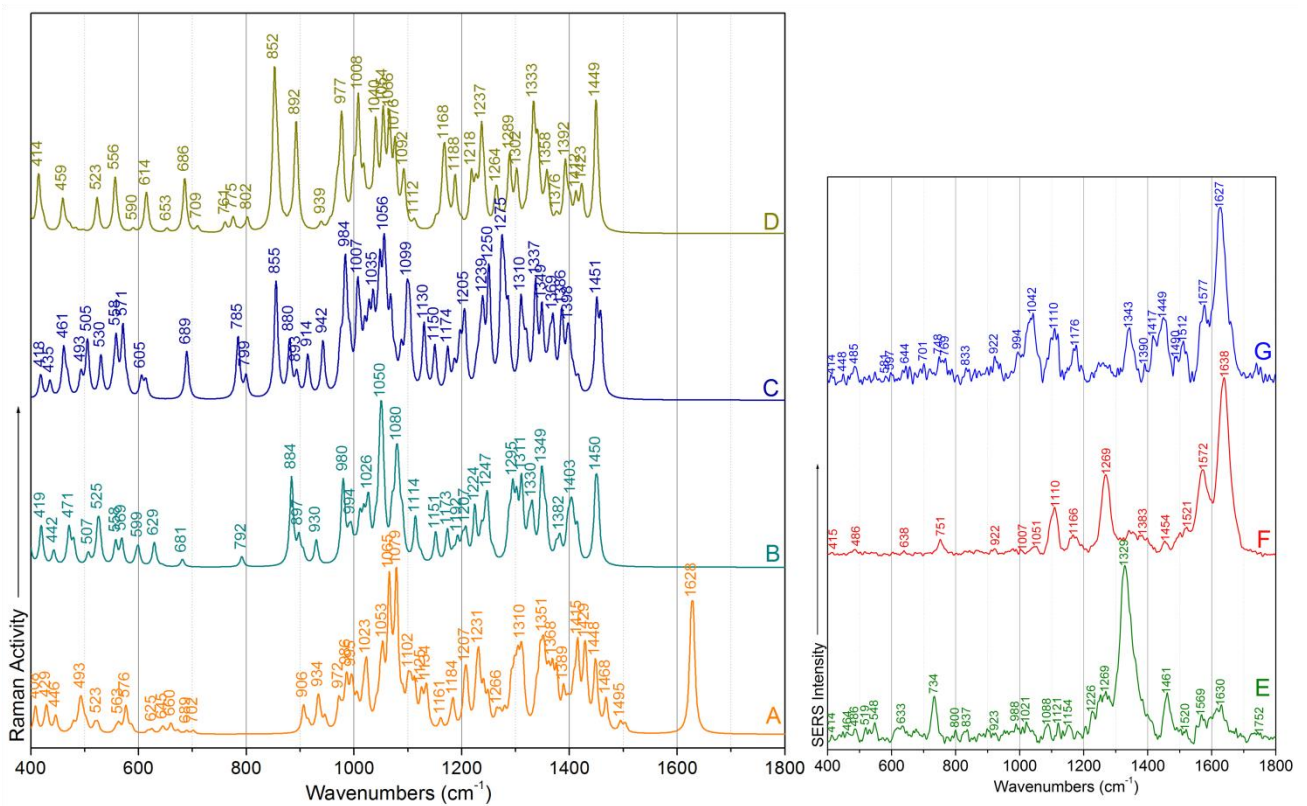


Figure 6 - Calculated Raman spectra of N-acetylglucosamine (A), β -1,3-glucan (B), β -1,6-glucan (C), and mannose (D); representative SERS spectrum for *C. parapsilosis* (E), *C. glabrata* (F), and *C. albicans* (G).

Table 5 – Assignments for the common SERS bands of *Candida* species as compared to the corresponding cell wall component(s), as obtained from DFT calculations performed at B3LYP/6-311++G(d,p) level of theory, in gas phase.

Experimental	Calculated	Molecule	Assignment
414-415	414	mannose	$\delta(\text{OH}) + \delta(\text{CH})$
	418	β -1,6-glucan	$\beta(\text{OCC}) + \delta(\text{OH}) + \delta(\text{CH})$ (in plane deformation of ring)
	419	β -1,3-glucan	$\beta(\text{COC}) + \delta(\text{CH}) + \delta(\text{OH})$ (in plane deformation of ring)
485-486	480	N-acetylglucosamine	$\delta(\text{NH}) + \text{ring breathing}$
633-644	646	N-acetylglucosamine	$\delta(\text{NH}) + \rho(\text{CH}_3) + \delta(\text{CH})$
701	709	mannose	$\beta(\text{OCO}) + \delta(\text{CH}) + \delta(\text{OH})$
	702	N-acetylglucosamine	$\beta(\text{OCO}) + \delta(\text{CH})$
734-751	761	mannose	$\beta(\text{CCC}) + \delta(\text{CH}) + \delta(\text{OH})$
800-806	802	mannose	$\beta(\text{OCC}) + \delta(\text{OH}) + \delta(\text{CH})$ (in plane deformation of ring)
	800	β -1,6-glucan	$\beta(\text{CCC}) + \delta(\text{OH}) + \delta(\text{CH})$
922-923	939	mannose	$\nu(\text{CC}) + \nu(\text{CO}) + \delta(\text{CH})$
	942	β -1,6-glucan	$\nu(\text{CO}) + \delta(\text{CH})$
	934	N-acetylglucosamine	$\rho(\text{CH}_2) + \nu(\text{OH})$ (intramolecular HB)
989-1007	990	β -1,3-glucan	$\nu(\text{CO}) + \delta(\text{OH}) + \delta(\text{CH})$
	997	N-acetylglucosamine	$\nu(\text{CO}) + \delta(\text{CH})$
1021-1042	1040	mannose	$\nu(\text{CC}) + \nu(\text{CO}) + \delta(\text{CH}) + \delta(\text{OH})$
	1024; 1024	N-acetylglucosamine	$\nu(\text{CO}); \nu(\text{CC}) + \nu(\text{CO}) + \delta(\text{CH}) + \delta(\text{OH})$
1088	1092	mannose	$\nu(\text{CC}) + \rho(\text{CH}_2) + \delta(\text{CH}) + \delta(\text{OH})$
	1088	β -1,6-glucan	$\nu(\text{CO}) + \nu(\text{CC}) + \delta(\text{CH}) + \delta(\text{OH})$
1110	1112	mannose	$\nu(\text{CO}) + \delta(\text{CH}) + \delta(\text{OH})$
	1114	β -1,3-glucan	$\nu(\text{CC}) + \nu(\text{CO}) + \rho(\text{CH}_2) + \delta(\text{CH}) + \delta(\text{OH})$
	1112	N-acetylglucosamine	$\nu(\text{CN}) + \nu(\text{CN}) + \delta(\text{NH}) + \delta(\text{CH}) + \delta(\text{OH})$
1121	1125	N-acetylglucosamine	$\nu(\text{CO}) + \nu(\text{CC}) + \delta(\text{CH})$
1224-1226	1226	mannose	$\tau(\text{CH}_2) + \delta(\text{CH}) + \delta(\text{OH})$
	1224	β -1,3-glucan	$\tau(\text{CH}_2) + \delta(\text{CH}) + \delta(\text{OH})$
1262-1269	1265	mannose	$\delta(\text{CH}) + \delta(\text{OH}) + \tau(\text{CH}_2)$
	1265	N-acetylglucosamine	$\delta(\text{CH}) + \delta(\text{OH})$
1329-1343	1333	mannose	$\delta(\text{CH}) + \delta(\text{OH})$
	1337	β -1,6-glucan	$\delta(\text{CH}) + \delta(\text{OH})$
	1331	β -1,3-glucan	$\delta(\text{CH}) + \delta(\text{OH})$
1383-1390	1392	mannose	$\delta(\text{CH}) + \delta(\text{OH}) + \omega(\text{CH}_2)$
	1386	β -1,6-glucan	$\delta(\text{CH}) + \delta(\text{OH})$
	1382	β -1,3-glucan	$\delta(\text{CH}) + \delta(\text{OH})$
	1389	N-acetylglucosamine	$\delta(\text{CH}) + \omega(\text{CH}_2)$
1449-1461	1449	mannose	$\beta(\text{CH}_2)$
	1450; 1458	β -1,6-glucan	$\beta(\text{CH}_2); \beta(\text{CH}_2)$ between rings
	1448; 1453	β -1,3-glucan	$\beta(\text{CH}_2); \beta(\text{CH}_2)$
	1447	N-acetylglucosamine	$\beta(\text{CH}_2)$
1520-1521	1495; 1504	N-acetylglucosamine	$\nu(\text{CN}) + \delta(\text{NH}) + \delta(\text{NH}); \nu(\text{CN}) + \delta(\text{NH}) + \delta(\text{CH})$
1627-1638	1626; 1630	N-acetylglucosamine	$\nu(\text{C=O}); \nu(\text{C=O}) + \delta(\text{NH})$

ν – stretching; β – bending; δ – out of plane bending; ρ – rocking; ω – asymmetric stretching; τ – twisting; HB – hydrogen bonding

REFERENCES

1. Oancea S, Stoia M. Rom Biotechn Letters 2010;15(5):5519-29.
2. A. H, al. e. Rom Biotechn Letters. 2013;18(6):8843-54.
3. Lode H. Clinic Microbiol Infection. 2005;11(10):778-87.
4. Girijala RL, Bush RL. Global Journal of Medicine and Public Health. 2017;6(1).
5. A H, S H, J C, al. e. Antimicrob Resist Infect Control. 2013;2(31).
6. Antimicrobial resistance: global report on surveillance. 2014.
7. RM K, JR E, Jr. RC, al. e. Public Health Rep. 2007;6:122-60.
8. Q L, Hao C, Xu Z. Sensors. 2017;17:627.
9. Chen J, al. e. Laser Phys Letters. 2016;13(10):105601.
10. Y. Z, al. e. Laser Phys Letters. 2016;13(6):065604.
11. K K, al. e. J Physics-Cond Matter, 14(18), 2002, R597-R624. 2002;14(8):R597-R624
12. Zhou H, Yang D, Ivleva NP, Mircescu NE, al. e. Analytical Chemistry. 2014;86(3):1525-33.
13. Zhou H, Yang D, Ivleva NP, Mircescu NE, Schubert S, Niessner R, et al. Label-Free in Situ Discrimination of Live and Dead Bacteria by Surface-Enhanced Raman Scattering. Analytical Chemistry. 2015;87(13):6553-61.
14. Zhou H, Yang D, Mircescu NE, al. e. Microchimica Acta. 2015;183(13):2259-66.
15. Mircescu NE, Zhou H, Leopold N, al. e. Anal Bioanal Chem. 2014;406(13):3051-8.
16. Dina NE, Zhou H, Colniță A, Leopold N, al. e. Analyst. 2017;142:1782-9.
17. Colniță A, Dina NE, Leopold N, Vodnar DC, Bogdan D, Porav SA, et al. Characterization and discrimination of gram-positive bacteria using Raman Spectroscopy with the aid of principle component analysis. Nanomat. 2017;7(9):248.
18. D. Yang HZ, N.E. Dina, C. Haisch. Royal Soc Open Sci. 2018;5(9):180955.
19. DINA NE, MARCONI D, Alia COLNIȚĂ, GHERMAN AMR. Microfluidic portable device for pathogens' rapid SERS detection. Proceedings. 2020;60(1):2.
20. Frisch MJ, Trucks HB, Schlegel HB, Scuseria GE, Robb MA, Cheeseman JR, et al. Gaussian 09, Revision B.01. Gaussian, Inc., Wallingford, CT, 2010; 2010.
21. Koopmans T. Über die Zuordnung von Wellenfunktionen und Eigenwerten zu den Einzelnen Elektronen Eines Atoms. Physical Review B: Condensed Matter. 1934;1(1-6):104-13.
22. Parr RG, Pearson RG. Absolute hardness: companion parameter to absolute electronegativity. Journal of American Chemical Society. 1983;105:7512-6.
23. Parr RG, Donnelly RA, Levy M, Palke WE. Electronegativity: The density functional viewpoint. Journal of Chemical Physics. 1978;68(8):3801.
24. Maynard AT, Huang M, Rice WG, Covell DG. Reactivity of the HIV-1 nucleocapsid protein p7 zinc finger domains from the perspective of density functional theory. Proceedings of the National Academy of Sciences of the United States of America. 1998;95:11578-83.
25. Parr RG, Szentpály Lv, Liu S. Electrophilicity Index. Journal of American Chemical Society. 1999;121:1922-4.

DISSEMINATION OF THE RESULTS

Papers on thesis' subject:

1. "Cheminformatic study on structural and bactericidal activity of latest generation β -lactams on widespread pathogens", **Ana Maria Raluca GHERMAN**, Nicoleta Elena DINA, Vasile CHIȘ, submitted paper at Pharmaceuticals (IF₂₀₂₁: 6.525; AI₂₀₂₁: 0.879; **Q1**)
2. "Finding specific spectral features for surface-enhanced Raman response of *Enterococcus faecalis* assisted by multivariate analysis when using common silver sols", Laurențiu STĂNCIOIU, **Ana Maria Raluca GHERMAN**, Nicoleta Elena DINA, Romanian Reports in Physics, 2021, 73 (4), 604 (IF₂₀₂₁: 2.085; AI₂₀₂₁: 0.202; **Q3**)
<http://www.rrp.infim.ro/2021/AN73604.pdf>
3. "Fuzzy characterization and classification of bacteria species detected at single-cell level by surface-enhanced Raman scattering", Nicoleta Elena DINA, **Ana Maria Raluca GHERMAN**, Alia COLNIȚĂ, Daniel MARCONI, Costel SÂRBU, Spectrochimica Acta, Part A, 2021, 247, 119149, DOI: 10.1016/j.saa.2020.119149 (IF₂₀₂₁: 4.831; AI₂₀₂₁: 0.491; **Q1**) (5 citations)
<https://www.sciencedirect.com/science/article/abs/pii/S1386142520311288>
4. "Identification of Salmonella serovars before and after ultraviolet light irradiation by Fourier Transform Infrared (FT-IR) Spectroscopy and Chemometrics", Cristina M. MUNTEAN, Nicoleta Elena DINA, Alexandra TĂBĂRAN, **Ana Maria Raluca GHERMAN**, Alexandra FĂLĂMAȘ, Loredana E. OLAR, Liora M. COLOBĂȚIU, Răzvan ȘTEFAN, Anal. Letters, 2021, 54 (1-2), 150-172, DOI: 10.1080/00032719.2020.1731524 – conference paper (IF₂₀₂₁: 2.267; AI₂₀₂₁: 0.230; **Q3**) (4 citations)
<https://www.tandfonline.com/doi/abs/10.1080/00032719.2020.1731524>
5. "Yeast cell wall – silver nanoparticles interaction: A synergistic approach between surface enhanced Raman scattering and computational spectroscopy tools", **Ana Maria Raluca GHERMAN**, Nicoleta Elena DINA, Vasile CHIȘ, Andreas Wieser, Christoph HAISCH, Spectrochimica Acta, Part A, 2019, 222, 117223, DOI: 10.1016/j.saa.2019.117223 (IF₂₀₁₉: 3.232; AI₂₀₁₉: 0.410; **Q1**) (8 citations)
<https://www.sciencedirect.com/science/article/abs/pii/S1386142519306134>
6. "Label-free detection of bacteria using Surface-Enhanced Raman Scattering and Principal Component Analysis", Ionuț Bogdan COZAR, Alia COLNIȚĂ, Tiberiu SZÖKE-NAGY, **Ana Maria Raluca GHERMAN**, Nicoleta Elena DINA, Analytical Letters, 2019, 52 (1), Special Issue, DOI: 10.1080/00032719.2018.1445747 (IF₂₀₁₉: 1.467; AI₂₀₁₉: 0.202; **Q3**) (5 citation)
<https://www.tandfonline.com/doi/full/10.1080/00032719.2018.1445747>
7. "Characterization of clinically relevant fungi via SERS Fingerprinting assisted by novel chemometric models", Nicoleta Elena DINA, **Ana Maria Raluca GHERMAN**, Vasile CHIȘ, Costel SÂRBU, Andreas WIESER, David BAUER, Christoph HAISCH, Analytical Chemistry 2018, 90 (4), 2484-2492, DOI: 10.1021/acs.analchem.7b03124 (IF₂₀₁₈: 6.35; AI₂₀₁₈: 1.348; **Q1**) (23 citations)
<https://pubs.acs.org/doi/10.1021/acs.analchem.7b03124>

Σ_{AI} : 2.883

6 (six) papers in ISI journals, out of which 2 (two) as first-author

1 paper submitted as first author in a journal with AI: 0.879

citations: 45

Conference participations on thesis' subject

Oral presentation:

1. 17th Scandinavian Symposium on Chemometrics (SSC17), "Inter- and intra-class discrimination based on multivariate analyses applied on bacterial SERS fingerprints", **Ana Maria Raluca GHERMAN**, Nicoleta Elena DINA, 6th-9th September 2021, Aalborg, Denmark
2. 12th International Conference on Processes in Isotopes and Molecules (PIM 2019), "*Principal Component Analysis as a discriminant tool. A case study on microorganisms*", **Ana Maria Raluca GHERMAN**, Vasile CHIȘ, Nicoleta Elena DINA, 25th – 27th September 2019, Cluj-Napoca, Romania
3. Prima Conferință Interdisciplinară pentru Studenți Doctoranzi, Babeș-Bolyai University, "*Accurate Prediction of Raman and NMR Spectra of Biomolecules*", **Ana-Maria-Raluca GHERMAN**, Vasile CHIȘ, 10th – 12th June 2016, Baru Mare, Hunedoara, Romania

Poster presentation:

1. 6th International Conference of Analytical and Nanoanalytical Methods for Biomedical and Environmental Sciences (IC-ANMBES 2022), "*Can molecular docking solely predict antibiotics' bactericidal activity?*", **Ana Maria Raluca GHERMAN**, Vasile CHIȘ, Nicoleta Elena DINA, 8th – 10th June 2022, Brașov, Romania – **BES Scholarship for Romanian students**
2. 11th International Conference on Processes in Isotopes and Molecules (PIM 2017), "*The bactericidal activity of some penicillins revealed by a synergistic approach between DFT and Raman Spectroscopy*", **Ana-Maria-Raluca GHERMAN**, Nicoleta Elena DINA, Silvia NEAMȚU, Vasile CHIȘ, 27th – 29th September 2017, Cluj-Napoca, Romania
3. 11th Triennial Congress of the World Association of Theoretical and Computational Chemists (WATOC 2017), "*Raman technique and Density Functional Theory – the 'R' & 'D' in Research and Development of antibiotics*" **Ana-Maria-Raluca GHERMAN**, Nicoleta Elena DINA, Ionuț Bogdan COZAR, Vasile CHIȘ, 27th August – 1st September 2017, München, Germany

6 (six) conference participations:

- 2 (two) oral presentations at international conferences
 - 1 (one) oral presentation at national conference
- 3 (three) poster presentations at international conferences